

# Joined Segmentation of Cortical Surface and Brain Volume in MRI using a Homotopic Deformable Cellular Model

Yann Cointepas, Isabelle Bloch  
ENST, Département TSI  
CNRS URA 820  
46 rue Barrault  
75634 Paris Cedex 13 FRANCE  
cointepa@tsi.enst.fr, bloch@tsi.enst.fr

Line Garnero  
LENA  
CNRS URA 654  
47 Bd de l'Hôpital  
75651 Paris Cedex 13 FRANCE  
lenalg@ext.jussieu.fr

## Abstract

*This paper presents a new method to segment both the brain volume and the cortical surface from a MR image of the head using a single model. This method is based on an original deformable model which can handle jointly volumes and surfaces using a cellular complex based representation. The model is initialized on the outer brain surface and then deformed inside the cortex folds according to both volumic and surfacic constraints, while preserving topology.*

## 1 Introduction

Segmentation of brain magnetic resonance (MR) images is a significant research field in medical imaging. However, the result of segmentation is, in general, only one stage in a more complex process like, for example, detection of pathologies, computer assisted surgery, or functional study of the brain. The aim of segmentation is to obtain a geometric representation of one or more structure. It is therefore necessary that the representation corresponds to the goals of the segmentation process. With regard to the segmentation of brain MR, and more particularly of the cortex, the various methods of segmentation can be roughly divided into two classes: surface methods and volume methods. Surface methods (e.g. [7, 8, 17]) are often based on deformable models and provide one or more surfaces that represent the limits between segmented objects. Most volume methods (e.g. [1, 13, 15, 18]) use a combination of different segmentation approaches (e.g. [2, 3]) like, for example: thresholding and clustering approaches, morphological approaches, knowledge based approaches, etc.

The segmentation of both the cortex surface and the brain volume is necessary for several applications including electroencephalography (EEG) and magnetoencephalography (MEG) studies. In order to regularize the inverse problem in EEG/MEG, it is necessary to build a model of cerebral structures of the subject or patient [6, 10, 14]. This model must allow the representation of both the cerebral volume and the surfaces which delimit this volume. This dual volumic and surfacic representation is difficult to obtain for the cortex surface because of the complexity of the cortical ribbon shape. The cortex is a thin part of grey matter of a few millimeters width located around the hemispheres. It presents many folds which form the sulci and the gyri. Inside the sulci, two distinct parts of the cortex are in contact. Therefore, cortex surface can be divided into two parts: the external surface which is the external surface of the hemispheres and the internal surfaces which are the parts of the cortex surface inside the folds (Figure 1).

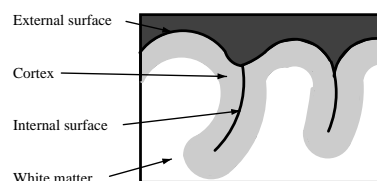


**Figure 1. Diagram of a cortex slice.**

Internal surfaces can disappear in MRI because of the partial volume effect. Therefore, a voxel based volumic segmentation cannot represent completely the cortical surface. On the other hand, surfacic segmentations methods can represent the cortex surface but do not give an explicit representation of the brain volume. In this paper, we introduce

a new segmentation method which is based on an original deformable model using cellular complexes structure and both surface and volume constraints. This modeling allows the representation of both the brain volume and the cortex surface in the same model. This is an original feature of our approach since, in contrary to purely 3-dimensional objects, the surface of the cellular model cannot be simply derived from the inner volume, neither the contrary. Therefore, neither volume methods nor surface methods solve the whole problem. In Section 2, we introduce the cellular deformable model. In Section 3, we present our segmentation method. Section 4 contains algorithmic considerations. The results are presented in Section 5. And Section 6 proposes a discussion about this method and future work.

## 2 Homotopic 3D cellular deformable model

The cellular model we propose is a 3-dimensional extension of an image representation proposed by Kovalevsky [12]. This representation is based on the structure of cellular complexes. A cellular complex is composed of cells of different dimensions. In the 3-dimensional case there are four different dimensions for the cells: 0-cells are points in  $\mathbb{R}^3$ , 1-cells are curves joining two 0-cells, 2-cells are surfaces which border is composed of 0- and 1-cells and 3-cells are volumes which border is composed of 0-, 1- and 2-cells.

A cellular complex only defines a few geometrical properties of the cells. To build the cellular model, which has to represent objects in  $\mathbb{R}^3$ , we must define the whole geometry of the cells (shapes, locations, orientations, etc.) in  $\mathbb{R}^3$  according to the MRI structure.

### 2.1 Cellular model

MR images are made up of voxels which are cubes or parallelepipeds in  $\mathbb{R}^3$ . In order to avoid to re-sample the MRI data, we build a structure that is close to the cubic grid. We represent all the parts of different dimensions which compose the voxel (Figure 2): 3-cells are cubes corresponding to the voxels, 2-cells are the facets of voxels, 1-cells are the segments that delimit the facets and 0-cells are the end points of segments.

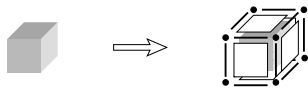


Figure 2. The cellular model

The cells are linked together by a connectivity relationship which forms a graph structure. Two cells are neighbors

(or connected) if one is part of the border of the other (this defines a symmetrical neighborhood relationship). For example, Figure 2 shows the neighborhood of a cube. Consequently, two cells of the same dimension are never directly connected. This model allows the representation of objects with different local dimensions (Figure 3). It is possible to represent objects composed of volumes, surfaces and curves.

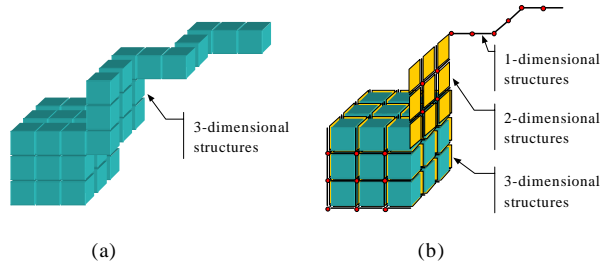


Figure 3. Representation of objects with different local dimensions. (a) Structures made up with voxels are always 3-dimensional. (b) Thin structures can be represented with a cellular model.

In addition to the modeling advantages of the cellular model, its topological properties allow us to build a homotopic deformable model.

### 2.2 Homotopic deformations of the cellular model

A scene represented with a cellular model can be deformed while keeping its initial topology. The homotopic deformations are based on the simple cells, which are cells that can be added or removed from the scene without changing its topology. We have shown that a local criterion can be used to detect simple cells [5]. This local criterion detects a simple cell according to its direct neighborhood: a cell is simple if and only if its neighborhood is composed of one object connected component and one background connected component (Figure 4). Therefore, it is possible to homotopically deform the model by iteratively modifying simple cells.

In the following section we present a cellular model based method to segment both the cortical surface and the volume of the hemispheres with the same model.

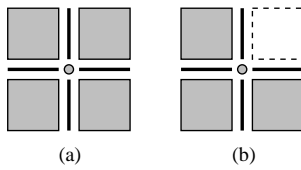


**Figure 4. 2-dimensional simple cells example. (a) The central point is not simple since there is no background connected component in its neighborhood. (b) One cell has been removed. The central point is simple and there is one object connected component and one background connected component in its neighborhood.**

### 3 Cortex segmentation

The segmentation process is based on a deformable model initialized on the external surface of the hemispheres and deformed towards the inside of the cortex gyri (Figure 5). The use of a cellular model gives a direct geometric representation of the cortical surface and of the hemispheres volume. Moreover, cellular models allows the use of homotopic deformation. It is thus possible to impose the initial model topology and preserve it during the deformation process. This property is important because the cortex has the same topology as a sphere. By preserving the topology during the deformation, the deformation space of the model is reduced and thus the complexity of the segmentation is decreased.

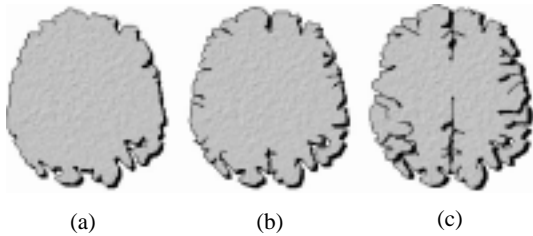


**Figure 5. Diagram of the deformation process. (a) The model is initialized on the external brain surface. (b) The model is "dug" towards the inside of the sulci. (c) Final state, the model surface is into the cortex folds and the initial topology is preserved.**

### 3.1 Cellular model initialization

To initialize the model it is necessary to segment the brain and the hemispheres. To segment the brain we use a method proposed by Mangin [13]. We developed a method to segment the brain stem, the cerebellum and the hemispheres in the segmented brain image. This method is based on mathematical morphology operators (Figure 6) and is not further detailed here. To impose the 3-dimensional model topology, we fill the 2-dimensional holes of the hemisphere volume slice by slice. We thus obtain an object with the same topology as a filled sphere. Then, the cellular model is initialized with the following algorithm:

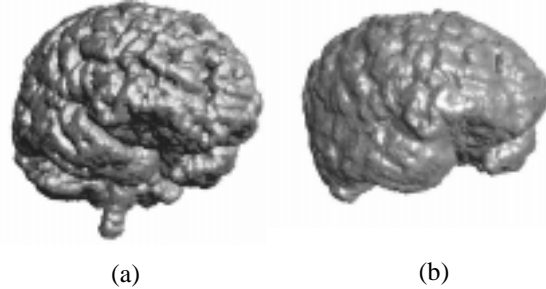


**Figure 6. 3-dimensional views (obtained with IDL) of the segmentation result for the brain (a) and for the hemispheres (b).**

To initialize the cellular model, we use the following algorithm:

```

Set all cells to the label background.

For each hemisphere voxel  $v$ :

    Set the cube corresponding to  $v$  and all its neighboring cells (which dimensions are lower than 3) to the label object.

End for

```

### 3.2 Cellular model deformation

To deform the cellular model, we must choose among the simple cells which ones can be modified in order to guide the model inside the cortex folds. The modification of a cell influences the "simpleness" of its neighbors. Therefore, the order in which the cells are modified is important because it can influence the segmentation result. This problem is common to all the deformation methods based on topology preserving deletion of elements like, for

example, homotopic thinning of a binary image [4, 11, 16]. But, with a cellular model, it is possible to reduce the effect of the traversing order. Indeed, two cells of the same dimension are never neighbors, therefore one can modify all the cells of a given dimension  $dim$  at the same time. The influence of the traversing order is not completely suppressed because the order in which the dimensions are traversed can influence the result. But the order effect does not privilege any traversing direction.

The model we use is composed of one object which is initialized on the hemispheres. Since the cortex is a part of the hemispheres, then the desired result is included in the initial object. Therefore, we only need to remove cells from the object during the deformation process. Hence, the deformation algorithm is the following:

```

For  $dim = 0$  to 3
  For each simple object cell  $s$  of dimension  $dim$ 
    If check_removal( $s$ ) is true
      remove  $s$  from the object
    End if
  End for
End for

```

The key point of the algorithm is the definition of the boolean function **check\_removal**. This function takes the decision to remove a cell from the object in order to guide the model towards the desired result. The removal decision is based on two types of information:

- Internal information which is obtained from the properties of the modeled object. This information allows us to guide the deformation according to geometric and topological properties of the modeled object.
- External information which is issued from a priori knowledge about the cerebral tissues and from measurements on the MRI.

These two types of information are detailed in the next sections.

### 3.2.1 Internal information

We use two different types of internal information. The first one, called evolution direction, is a set of local vectors located on the model surface and oriented in the direction which the model should take according to the surface shape. The second information is a local criterion used to regularize the surface shape.

### Evolution direction

Cortical topology allows us to use the cortex surface to estimate the direction of the folds. Indeed, the parts of the cortex folds which are close to the outer cortex surface are oriented in a direction close to the normal of this surface. While moving away from this surface, the direction may change, although not drastically [7]. It is therefore necessary to distinguish external surface and internal surfaces to define the evolution directions. The evolution directions of the external surface are normal to this surface, whereas the evolution directions of the internal surfaces are locally tangent to these surfaces at their border (Figure 7).

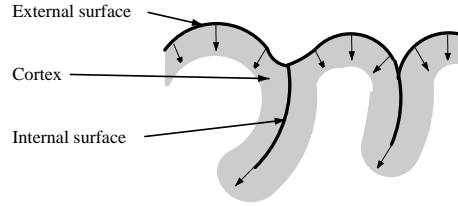


**Figure 7. Diagram of the evolution directions of the model surface.**

We developed an algorithm to compute an evolution direction for each facet (i.e. 2-cell) belonging to the model surface. This algorithm is made of two stages: in the first one a local direction is computed for each facet, in the second stage these local directions are smoothed along the model surface. To compute the local direction between two cells, the algorithm uses the centers of the cells, we denote  $center(s)$  the gravity center of a cell  $s$ . The computation of the local evolution direction for a facet  $f$  is done with the following algorithm:

```

 $result = \text{null vector}$ 
For each neighbor  $s$  of  $f$ 
  If  $s$  is an object cube
     $result = result + (center(s) - center(f))$ 
  Else if  $s$  is a segment and there is no facet of the
  surface, except  $f$ , in the neighborhood of  $s$ 
     $result = result + (center(s) - center(f))$ 
  End if
End for
Normalize  $result$ 

```

The first condition in this algorithm is used to compute the local direction for the facets of the external surface. Such facets have only one object cube in their neighborhood, this cube allows the detection of the object interior. Therefore, the local evolution direction for an external facet is normal to the facet and directed towards the interior of the model.

The second condition detects the borders of internal surfaces. Each border adds a contribution to the facet to which it belongs. The contribution of all the borders of one internal facet are added to compute the local evolution direction of this facet (Figure 8).

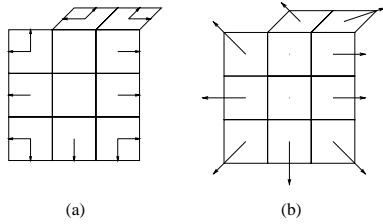


**Figure 8. Computation of local directions for an internal surface. (a) Each border of the surface adds a contribution to the direction of the facet to which it belongs. (b) Local directions resulting from the borders contributions. Facets which are not on the border have null local directions**

The evolution directions need to be less local than the local directions in order to take into account the surface shape. Therefore, we compute, for each surface facet, the mean of the local directions on a geodesic neighborhood along the surface. The “smoothed” directions obtained are the evolution directions. These directions are used jointly with external information to guide the deformations (Section 3.2.2).

### Regularization

The purpose of the second type of internal information is to regularize the shape of the internal surface. Indeed, if the deformations were not constrained enough, the surface could evolve in many directions and thus it could present a lot of irregularities. To limit this problem, we prevent the internal surfaces to split into several branches by imposing that a segment cannot be neighbor to more than two surface facets. This condition is used directly in the algorithm which decides to remove an object cell.

### 3.2.2 External information

External information is used to combine the information given by the MR image and the a priori knowledge about the cortical topology. This information is used to guide the model deformation inside the cortex sulci and is expressed as cost functions which are combined together to take the final decision (section 3.2.3). Three different pieces of external information are used:

- A classification is used on the hemisphere image to build a membership to the cortex for each cube of the model.
- We use the hypothesis that the cortex width is almost constant to guide the internal surfaces in the cortex folds. We thus build a function which evaluate the cortex width around an internal facet.
- The location of the cerebro-spinal fluid (CSF) inside the brain is a good indicator of the cortex surface location. The brain is immersed into the CSF and the CSF goes into the cortex gyri. Therefore, we use the CSF inside the gyri to guide our model.

#### Membership to the cortex

To make some measurements on the cortex, we build an image which represents the membership value to the cortex for each voxel of the hemisphere volume. To build this image, we perform a grey level based classification of the brain image with the k-means algorithm, then we extract the cortex label and apply a mean filter to account for imprecision on the cortex delineation (Figure 9). The membership to the cortex ( $\mu_{cortex}$ ) is normalized between 0 and 1. It is used directly to take the decision to remove a cube from the model: if the membership to the cortex of a cube is too low, the cube is removed. Thus, the object is being dug where the sulci are wide enough to appear on the MRI. We also use  $\mu_{cortex}$  to evaluate the cortex width around an internal facet.

#### Cortex width

In MRI, the cortical surface can disappear because of the partial volume effect. Under the hypothesis that the cortex width is almost constant, these locations can be detected because they are about twice wider than the cortex (Figure 10). The detection of the wide structures is used to guide the deformations of the internal surfaces into the sulci. To do this we build a cost function ( $\mu_{width}$ ) which indicates if an internal facet  $f$  is in a wide structure or not. This function represents the smallest cortex width around the facet:

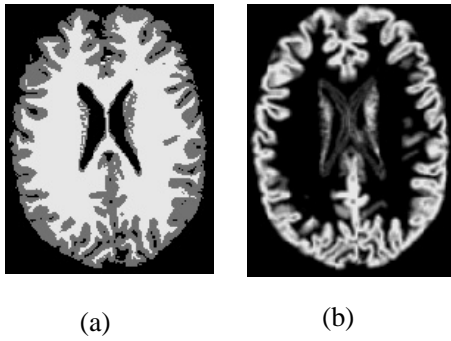


**Figure 9. Slice of a 3D volume. (a) Classification of the hemispheres image. (b) Image of the membership to the cortex ( $\mu_{cortex}$ ).**

$$\mu_{width}(f) = \min_{\vec{d} \in \{\vec{n}, -\vec{n}, \vec{e}\}} cwidth(center(f), \vec{d}, l)$$

where :

$l$  is an estimation of the cortex width

$\vec{n}$  is a normal to  $f$

$\vec{e}$  is the evolution direction of  $f$

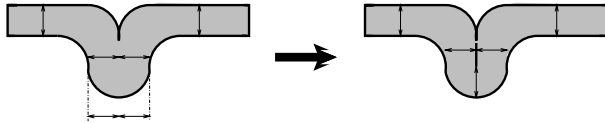


**Figure 10. Diagram of the cortical ribbon. On the left, the object presents a structure twice wider than the rest of the ribbon. On the right, the surface of the cortex has been prolonged to make the ribbon width constant.**

The function  $cwidth(p, \vec{d}, l)$  evaluates the cortex thickness along the segment starting at point  $p$  with a length  $l$  in the direction  $\vec{d}$ . This value is obtained by calculating the mean value of  $\mu_{cortex}$  along the segment. If the segment is not completely in the object (for example if it is across an internal facet) then only the point of the segment located between  $p$  and the obstacle are considered. We use the following algorithm to calculate  $cwidth(p, \vec{d}, l)$ :

$$result = 0$$

$t =$  length of the smallest edge of a voxel of the MRI (voxels are often not cubic)

$points =$  sampling of the segment  $(p, \vec{d}, l)$  with a step  $t$

If the segment  $(p, \vec{d}, l)$  is across a background cell, then keep only the object points of the segment which are connected to  $p$

For each point  $q$  in  $points$

Project  $q$  in the image of the membership to the cortex and add the value to  $result$

End for

$$result = \frac{result}{t}$$

### Location of cerebro-spinal fluid in sulci

The last external information used to guide the model deformation is based on the detection of the cerebro-spinal fluid into the cortex sulci. To detect the CSF located in the sulci, we use a method proposed by Géraud [9] which is based on watershed and mathematical morphology operators (Figure 11).

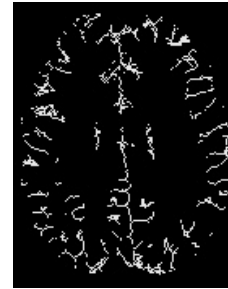


**Figure 11. Detection of the cerebro-spinal fluid located into the sulci.**

The CSF image ( $csf$ ) is used to build a cost function  $\mu_{csf}$  which represents the mean value of CSF in the neighborhood ( $N_O$ ) of a facet  $f$ :

$$\mu_{csf}(f) = \frac{\sum_{v \in N_O(f)} csf(v)}{|N_O(f)|}$$

The two functions  $\mu_{cortex}$  and  $\mu_{csf}$  are combined together in a weighted sum to take the decision to remove an internal facet. This is detailed in the following section.

### 3.2.3 Decision algorithm

The function **check\_removal**, introduced in section 3.2, makes the distinction between three simple cell types. Each cell type has its own removal criterion:

- A simple cell which belongs to the surface of the object is always removed. This is done because if one wants to dig into an object, one must dig through its surface first. If the 0-, 1- and 2-cells composing the object surface were not removed, one could not dig into the model while preserving its topology.
- A simple cube  $c$  is removed if  $\mu_{cortex}(c)$  is lower than a given threshold  $s_{volume}$ . When the sulci are wide enough, they contain cerebro-spinal fluid. In the MRI, the CSF is darker than the cortex and therefore the  $\mu_{cortex}$  value of the CSF voxels is low. Hence, by removing the cubes with low  $\mu_{cortex}$  values, the model is deformed inside the folds that are large enough to contain CSF voxels.
- In the places where the cortex folds are tightened, the cortical surface disappears from the MRI due to partial volume effect. To guide the internal surfaces inside the sharp parts of the sulci, we use two kinds of external information:  $\mu_{width}$  and  $\mu_{csf}$ . An internal facet  $f$  is removed if  $(1 - \alpha) \cdot \mu_{width}(f, l) + \alpha \cdot \mu_{csf}(f)$  is greater than a given threshold  $s_{surface}$  and if the regularization criterion is true (see Section 3.2.1 above). The values  $l$  and  $\alpha$  are parameters of the algorithm.  $l$  is an estimation of the cortex width and is used evaluate the cortex width around the facet  $f$  (see section 3.2.2 above).  $\alpha$  is used to select the importance of  $\mu_{width}$  and  $\mu_{csf}$  in the guiding process.

The deformation algorithm is rather short but the amount of data contained by a cellular model imposes to optimize its implementation.

## 4 Implementation considerations

It is possible to use a simple array as a data structure to represent a cellular model [5]. Such a structure has two main advantages. On the one hand, the array contains only information about the cells. No memory is used to represent the relationship between the cells. Therefore, this is an optimal representation for memory usage. As a result, a cellular model based on a 3-dimensional image uses eight times the amount of memory used by the image. On the other hand, the neighborhood relationships are represented as offsets in the array. Hence, almost no computing time is needed to traverse the graph structure of the cellular model. As a result, the significant computing time of the cellular model based algorithm is not increased because of the implementation. Therefore, one can build fast algorithms in spite of the amount of data used by the cellular model.

The data structure used to represent a cellular model gives the possibility to optimize the deformation algorithm which heavily uses the neighborhood relationship. For example, we reduced by ten the time of the simple cell detection algorithm by using offsets arrays representing frequently used neighborhood structures. Moreover, the deformation algorithm considers only simple cells which are much fewer than the total cell number because they are, by definition, located at the limit between the object and the background. When a simple cell is modified by this algorithm, only the neighboring cells are influenced by this modification. Therefore, the deformation process is fast enough to be implemented on actual computers.

The segmentation process is more time consuming than the raw deformation process. This is due to the computing of the information needed to guide the model towards the desired result. Most of the algorithm time is spent in computing the evolution direction and in evaluating the cortex width. As a result, it is therefore necessary, when building a process based on homotopic deformation of a cellular model, to take into account the intensive use of the guiding criteria in the deformation algorithm. Therefore, only fast computing criteria can be used. As an example, the full segmentation process (i.e. brain segmentation, hemispheres segmentation and cortex segmentation) for a MR image of the head takes approximatively two hours and half on a Sun Ultra-2 workstation.

## 5 Results

To present the results and evaluate the localization of the model surface in the brain, we developed a visualization tool allowing the superimposition of the model surface on an image slice. This method displays, over the slices, the surface facets (either internal or external) which are located in the slice and which are perpendicular to it. We present the surface superimposed on the membership to the cortex image in order to visualize the model surface location as compared to the cortex folds locations.

Figure 12 presents the results on a part of the brain. It shows the model evolution at different steps of the algorithm. One step corresponds to the traversing of all the simple cells of the model. The surface topology is preserved during the deformation process. Although the resulting model surface is irregular and seems to be disconnected on the 2-dimensional slices, the 3-dimensional connectivity is preserved (it is difficult to see on a 2-dimensional representation). Unfortunately, irregularities on the surface

prevent the use of a 3-dimensional visualization.

The segmentation algorithm uses several parameters which influence the results. The threshold  $s_{volume}$  on the membership to the cortex is quite easy to select because it can be visually selected on  $\mu_{cortex}$  image and because small modifications on  $s_{volume}$  do not change the results drastically. The three other main parameters are used to guide the deformations of internal surfaces. They are linked together and therefore their tuning is more difficult than the one of  $s_{volume}$ . The estimated cortex width  $l$  must represent a compromise between detection and regularization. If it is too small, the internal surfaces are more sensitive to small structures with high  $\mu_{cortex}$ , therefore the internal surfaces are more sensitive to noise. If  $l$  is too large, some sulci cannot be detected by the deformation algorithm. The weight  $\alpha$  represents the compromise between guidance on CSF and guidance on cortex width. If  $\alpha = 1$ , the internal surfaces are only guided by the detection of CSF in the sulci, whereas if  $\alpha = 0$ , only the detection of wide cortex structures guides the surfaces. A good compromise is  $\alpha \simeq 0.7$  because lower values makes more irregular surfaces. The threshold  $s_{surface}$  is also set according to a compromise between noise and detection. The results of Figure 12 were obtained with the following values:  $s_{volume} = 0.3$ ,  $s_{surface} = 0.65$ ,  $\alpha = 0.7$  and  $l = 4mm$ .

## 6 Discussion

In this paper, we presented a new segmentation method based on an original deformable model. We built a homotopic deformable model based on the cellular complex structure. Such a model allows to represent and to deform complex objects composed of structures with different local dimensions. Cellular model based representations give a direct 3-dimensional tessellation of both the volumes and the surfaces of the modeled objects. The use of a homotopic cellular deformable model is well adapted to the segmentation of complex objects which have a known topology, such as the cortical ribbon.

The segmentation results present a good localization of the cortex surface in both the wide and the thin parts of the sulci. The guiding criteria allow a good detection of the cortex surface. However, the resulting surface is irregular, it is therefore necessary to introduce a more robust regularization method in the deformation algorithm. The regularization could be based, for example, on discrete differential geometry operators in order to introduce constraints on curvature and on torsion.

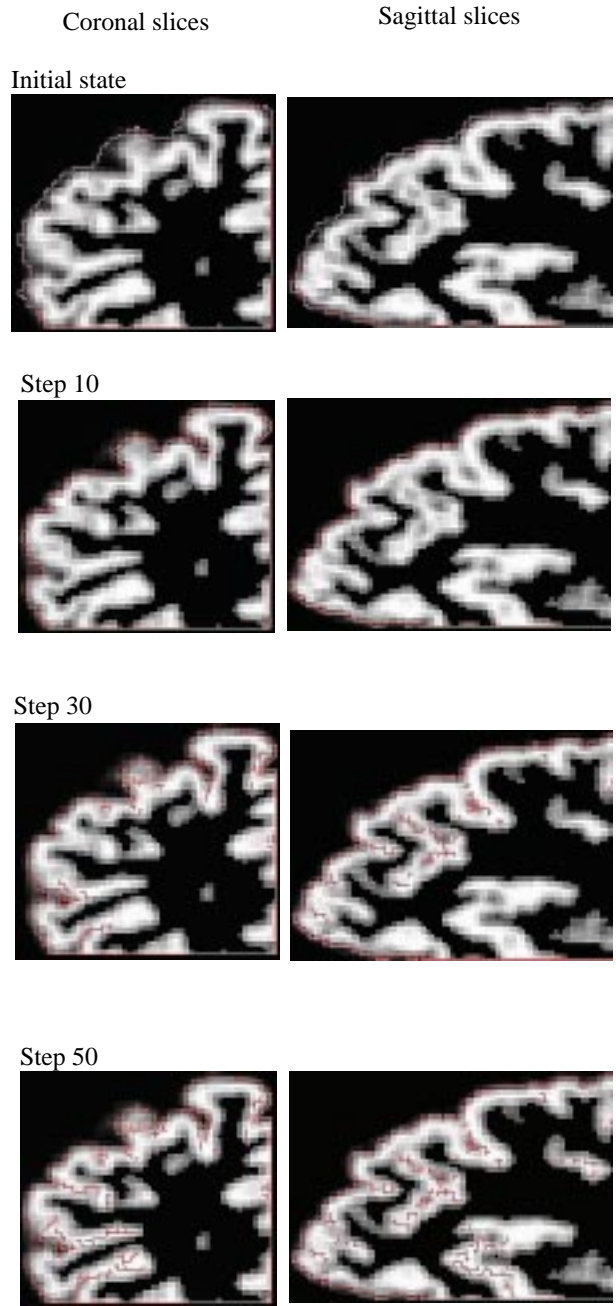


**Figure 12. Model evolution during the segmentation process. Parameters are:**  $s_{volume} = 0.3$ ,  $s_{surface} = 0.65$ ,  $\alpha = 0.7$  and  $l = 4mm$ .

The cellular deformable model based segmentation can be useful in several domains. For example, a tessellation of the cerebral tissues which is both volumic and surfacic is useful for solving the direct problem in EEG and MEG.

Moreover, in this framework, a realistic model of the cortical surface can be used to regularize the inverse problem by computing some geometrical values such as normals to the surface and geodesic distances along the surface.

## References

- [1] P. Allain, J. Travère, D. Bloyet, J. Baron, and M. Devignes. Segmentation entièrement automatique du volume cérébral observé par résonance magnétique. In *Proceedings GRETSI*, pages 1275–1278, Juan-les-pins, France, Sept. 1993.
- [2] L. Aurdal. *Analysis of multi-image magnetic resonance acquisitions for segmentation and quantification of cerebral pathologies*. PhD thesis, Ecole Nationale Supérieure des Télécommunications, 1997.
- [3] N. Ayache. L'analyse automatique des images médicales état de l'art et perspectives. Technical Report 3364, INRIA, Sophia-Antipolis, Feb. 1998.
- [4] G. Bertrand and G. Malandain. A new characterization of three-dimensional simple points. *Pattern Recognition Letters*, 15:169–175, Feb. 1994.
- [5] Y. Cointepas, I. Bloch, and L. Garnero. A discrete homotopic deformable model dealing with objects with different local dimensions. In *Discrete Geometry for Computer Imaging*, pages 258–271, Noisy-le-Grand, France, Mar. 1999.
- [6] A. M. Dale and M. I. Sereno. Improved localization of cortical activity by combining EEG and MEG with MRI cortical surface reconstruction: A linear approach. *Journal of Cognitive Neuroscience*, 5(2):162–176, 1993.
- [7] C. Davatzikos. Using a deformable surface model to obtain a shape representation of the cortex. *IEEE Transactions on Medical Imaging*, 15(6):785–795, Dec. 1996.
- [8] H. Delingette. General object reconstruction based on simplex meshes. Technical Report 3111, INRIA, Sophia-Antipolis, Feb. 1997.
- [9] T. Géraud. *Segmentation des structures internes du cerveau en imagerie par résonance magnétique tridimensionnelle*. PhD thesis, Ecole Nationale Supérieure des Télécommunications, June 1998. (ENST 98 E 012).
- [10] M. Hämäläinen, R. Hari, R. J. Ilmoniemi, J. Knuutila, and O. V. Lounasmaa. Magnetoencephalography theory, instrumentation and applications to noninvasive studies of the working human brain. *Reviews of Modern Physics*, 65(2):413–497, Apr. 1993.
- [11] T. Y. Kong and A. Rozenfeld. Digital topology: Introduction and survey. *Computer Vision, Graphics, and Image Processing*, 48:357–393, 1989.
- [12] V. A. Kovalevsky. Finite topology as applied to image analysis. *Computer Vision, Graphics, and Image Processing*, 46:141–146, 1989.
- [13] J.-F. Mangin. *Mise en correspondance d'images médicales 3D multi-modalités multi-individus pour la corrélation anatomo-fonctionnelle cérébrale*. PhD thesis, Ecole Nationale Supérieure des Télécommunications, Mar. 1995. (ENST 95 E 010).
- [14] B. Renault and L. Garnero. L'imagerie électromagnétique cérébrale, principe de base et perspectives. *Colloque de l'Académie des Sciences : Instrumentation physique en biologie et en médecine*, pages 131–139, Dec. 1994.
- [15] H. Rifai, I. Bloch, S. Hutchinson, J. Wiart, and L. Garnero. Segmentation of the Skull in MRI Volumes Using Deformable Model and Taking the Partial Volume Effect into Account. *Medical Image Analysis (to appear)*, 1998.
- [16] P. K. Saha, B. Chanda, and D. D. Majumder. Principles and algorithms for 2-D and 3-D shrinking. Technical report, Indian Statistical Institute, Calcutta, 1991.
- [17] D. J. Schlesinger, J. W. Snell, L. E. Mansfield, J. R. Brookeman, J. M. Ortega, and N. F. Kassel. Segmentation of volumetric medical imagery using multiple geodesic-based active surfaces. SPIE Medical Imaging'96, 1996.
- [18] C. Tsai, B. Manjunath, and R. Jagadeesan. Automated segmentation of brain MR images. *Pattern Recognition*, 28:1825–1837, 1995.